



# Self-compacting concrete containing coarse recycled precast-concrete aggregate and its durability in marine-environment-related tests

Francisco Fiol<sup>a</sup>, Víctor Revilla-Cuesta<sup>b,\*</sup>, Carlos Thomas<sup>c</sup>, Juan M. Manso<sup>a</sup>

<sup>a</sup> Department of Construction, Escuela Politécnica Superior, University of Burgos, c/ Villadiego s/n, 09001 Burgos, Spain

<sup>b</sup> Department of Civil Engineering, Escuela Politécnica Superior, University of Burgos, c/ Villadiego s/n, 09001 Burgos, Spain

<sup>c</sup> LADICIM (Laboratory of Materials Science and Engineering), E.T.S. de Ingenieros de Caminos, Canales y Puertos, Universidad de Cantabria, Av./ Los Castros 44, 39005 Santander, Spain

## ARTICLE INFO

### Keywords:

Recycled precast-concrete aggregate  
Self-compacting concrete  
Marine environment  
Capillary water absorption  
Carbonation  
Moist/dry test

## ABSTRACT

Marine environments are extremely challenging for the long-term durability of concrete. Prior validation of concrete durability is therefore a prerequisite to guarantee its adequate performance under marine environmental conditions. In this study, the performance of Self-Compacting Concrete (SCC) with variable contents of coarse Recycled Precast-Concrete Aggregate (RPCA) and two different cement contents is assessed in terms of capillary water absorption, natural and accelerated carbonation, resistance to SO<sub>2</sub> attack, and moist/dry performance in drinking water, marine water, and sulfate water. These tests are intended to simulate the conditions of a marine environment. In general, the results showed that an SCC containing coarse RPCA of adequate durability under marine conditions could be produced. On the one hand, porosity due to the presence of RPCA increased less as the cement content was increased, which in turn reduced water absorption and SCC carbonation. For example, the effective porosity of the SCC was reduced by 25 % between day 28 and day 180, following the addition of 100 % coarse RPCA. On the other hand, both the SO<sub>2</sub>-attack and the moist/dry tests revealed that the weight of the SCC with RPCA underwent greater variations, due to the reactions of the cement-hydration products with chlorides and sulfates, as well as salt deposition. However, SCC compressive strength was never adversely affected, as the concrete strength increased up to 8 MPa after the drinking-water and the sulfate-water moist/dry tests when using RPCA. According to both Fick's and Parrot's models, the projected service life of all the mixes was over 100 years, regardless of the coarse RPCA content, making this sort of SCC a feasible option for construction in marine environments.

## 1. Introduction

Nowadays, concrete is the most widely used civil-engineering construction material. It can be shaped in almost any form when fresh and its adequate strength, obtained at reasonable cost, make it the ideal material for many construction projects throughout the world [1,2]. However, it is also true that raw material production and concrete manufacturing harm the environment, especially so with regard to cement and aggregate. Cement is fundamentally harmful to the environment in terms of CO<sub>2</sub> emissions, as the production of one ton of cement emits between 0.9 and 1 ton of CO<sub>2</sub> into the atmosphere [3]. The aggregate-extraction process can also cause significant environmental damage in the form of quarries and gravel pits that modify water flows, patterns of land erosion, and vegetative cover, with negative impacts on

flora, fauna, and local micro-habitat [4]. Therefore, one of the main concerns of the concrete sector is concrete sustainability and how it can be increased, particularly through strategies to promote sustainable raw materials [5,6] that are often extracted from waste products. A process that implies the recovery of materials that might otherwise be dumped at landfill sites [7,8].

One of the best known and most widely studied improvements to concrete sustainability is the use of crushed concrete components as a substitute for Natural Aggregate (NA) [9,10]. Known as recycled aggregate, this material at adequate dosages can be used in concrete mixes, as long as the crushing is conducted in such a way that its particle size distribution is continuous [11]. The reject concrete components are recycled into aggregate particles that are nothing other than the same materials that constituted the parent concrete. Thus, both NA and

\* Corresponding author.

E-mail address: [vrevilla@ubu.es](mailto:vrevilla@ubu.es) (V. Revilla-Cuesta).

<https://doi.org/10.1016/j.conbuildmat.2023.131084>

Received 4 October 2022; Received in revised form 4 March 2023; Accepted 16 March 2023

Available online 23 March 2023

0950-0618/© 2023 The Author(s). Published by Elsevier Ltd. This is an open access article under the CC BY-NC-ND license (<http://creativecommons.org/licenses/by-nc-nd/4.0/>).

cementitious matrix can be identified in the coarse particles [12,13]. The smaller particles can be fine particles of NA or small particles of crushed cementitious matrix [14]. This composition means that recycled aggregate is of a lower density, similar to the density of concrete ( $2.4 \text{ Mg/m}^3$ ), and has higher water absorption levels than NA, reaching 12 % in the finer fractions [14,15].

The composite nature of recycled aggregate and its physical properties condition the concrete to which it is added and its behavior. Thus, concrete containing recycled aggregate has lower levels of workability and mechanical strength [16,17], while its deformability under loading is higher [18,19]. The function of the concrete designer should therefore be to minimize these negative effects, adjusting the recycled aggregate content and the proportion of the other components of the concrete mix, such as the water-to-cement ratio, at all times seeking a balance between workability and mechanical behavior [20]. If this design principle is followed, it has been proven in the scientific literature that recycled aggregate can be used for the production of structural concrete [21]. The use of Recycled Precast-Concrete Aggregate (RPCA) is also beneficial. RPCA is produced at precast-concrete companies from reject concrete components that are crushed. RPCA improves the performance of the concrete in which it is incorporated compared to conventional recycled aggregate [22], due to the high strength of the cementitious matrix and the quality of the NA embodied in the RPCA [23], although the need for an adequate mix design must always be borne in mind [20].

The high flowability of Self-Compacting Concrete (SCC) makes it useful in many applications. With no need for vibration, SCC can be adapted to complex formworks and pumped to high heights [24]. Furthermore, it increases output and decreases energy costs at precast-concrete plants [22]. The design of this type of concrete requires a high content of fine particles and the addition of plasticizing admixtures, so that the flow of cement paste can drag the aggregate particles along with it [25,26]. The addition of recycled aggregate to SCC has the same effects on its behavior as conventional concrete [24], although this type of concrete usually requires high amounts of fine aggregate that implies a meticulous study of the quantity of fine RPCA fraction that should be added [27,28]. An adequate performance of SCC containing RPCA requires a mix design that enumerates the right quantity of this alternative aggregate and a suitable water-to-cement ratio [20].

Two key aspects determine concrete durability: porosity and the Interfacial Transition Zones (ITZ), *i.e.*, the aggregate/cementitious matrix bonding zones. On the one hand, porosity conditions the entry of external aggressive agents, which can cause internal damage and corrode reinforcements within a concrete matrix [29,30]. On the other hand, both the strength and the density of the ITZ must be adequate, as the higher the quality of the ITZ, the greater the difficulty of any aggregate detaching itself from the matrix, due to such phenomena as freezing/thawing and salt crystallization [31,32]. Any type of recycled aggregate, including RPCA, generally worsens both porosity and ITZ density and likewise concrete durability [33]. First, it increases the porosity of the cementitious matrix, a phenomenon that is particularly noticeable when the fine fraction of this sustainable aggregate is used [14]. Secondly, it weakens the ITZ due to the existence of bonds between the cementitious matrix of the new concrete and the cementitious matrix of the parent concrete [34,35]. These phenomena are usually aggravated in SCC by its high proportion of cement paste [24], which usually causes a more pronounced increase in the porosity of the cementitious matrix [36].

The marine environment is, together with extreme cold conditions, the most challenging for concrete in terms of its durability [37], due to the confluence of two aspects: high ambient relative humidity, and highly saline seawater in which the concrete is submerged [38,39]. Industrial concrete constructions in ports and seawalls are also demanding in terms of their durability, as there may be chemical products, such as sulfur dioxide, that will alter the mechanical performance of concrete due to their reaction with the chemical compounds that compose the cementitious matrix [40]. Despite its relevance, the study of the

durability behavior of concrete containing recycled aggregate in a marine environment is an under-researched area of the literature, although the use of very high contents of recycled aggregate in concrete has been shown to lead to worse degradation under those environmental conditions than in concrete containing NA [40,41]. Focusing on SCC made with RPCA, there are no available studies. For this reason, the analysis of the durability behavior of an SCC with that aggregate type is included in this study. An SCC with variable coarse RPCA content (0 %, 20 %, 50 % and 100 %) was tested to assess its durability in marine environment. The tests were designed to simulate the different marine conditions to which the concrete can be subjected, such as capillary-water-absorption test,  $\text{SO}_2$ -attack test, carbonation test, and moist/dry tests in drinking water, marine water, and sulfate water. The conducted moist/dry tests were aimed to analyze the long-term behavior of concrete, which are very scarce in the literature for any concrete type. The ultimate objective is to demonstrate that an SCC made with a sustainable quality aggregate such as RPCA and following a suitable mix design can be successfully used under marine conditions.

## 2. Materials and methods

### 2.1. Raw materials

All the conventional raw materials used in the manufacture of the concrete mixes were supplied from a precast-concrete plant that collaborated in this research, so the SCC mixes that were tested in this study used the same raw materials found in industrial concrete components. A CEM I 52.5 R cement as per EN 197-1 [42] (density of  $3.12 \text{ Mg/m}^3$  and Blaine specific surface of  $365 \text{ m}^2/\text{g}$ ); limestone filler  $<0.063 \text{ mm}$  (96.5 %  $\text{CaCO}_3$  by weight), to increase the content of aggregate fines within the mix; and two admixtures, a water-entrainment agent (proportion of 0.5–1 % of the cement mass) and a plasticizer (between 0.5 % and 1.5 % of the cement mass), for adequate fresh flowability of SCC without excessively increasing the water content. Two different fractions of NA were used: sand (0/2 mm) and gravel (2/12.5 mm). Both were of a rounded siliceous nature, an aggregate type commonly used in SCC, because its oval shape is easily dragged within the cement paste [26,43].

The coarse RPCA, size 4/12.5 mm, was produced from reject concrete components due to dimensional errors that could not be commercialized. To do so, hydraulic clamping broke the components into fragments, so that the reinforcements could be removed, and the concrete fragments were subsequently subjected to a two-stage crushing process using jaw crushers (final size of the concrete fragments of 0/150 mm) and impact crushers (concrete fragments with a final size of 0/30 mm). Finally, sieving reduced the aggregate to the required size of 4/12.5 mm. The crushed concrete components were manufactured with the raw materials described in the previous paragraph and had a compressive strength between 30 and 50 MPa.

The particle size of all the aggregates is shown in Fig. 1, which was continuous in all cases. Coarse RPCA had a lower density and higher water absorption levels than siliceous gravel (Table 1), in accordance with what is widely reported in the literature [14,24].

### 2.2. Mix composition

First, two control SCC mixes were produced with 0 % coarse RPCA, in which the proportions of the raw materials used in the SCC mixes manufactured at the precast-concrete plant were maintained. The difference between them was the target compressive strength of 30 MPa and 45 MPa, respectively. Thus, the effect of RPCA on SCC was analyzed on the basis of the SCC compositions used by the collaborating company. Subsequently, 20 %, 50 %, and 100 % coarse RPCA was incorporated in each control mix, in substitution of siliceous gravel. The incorporation of coarse RPCA led to a change in the added amount of two raw materials:

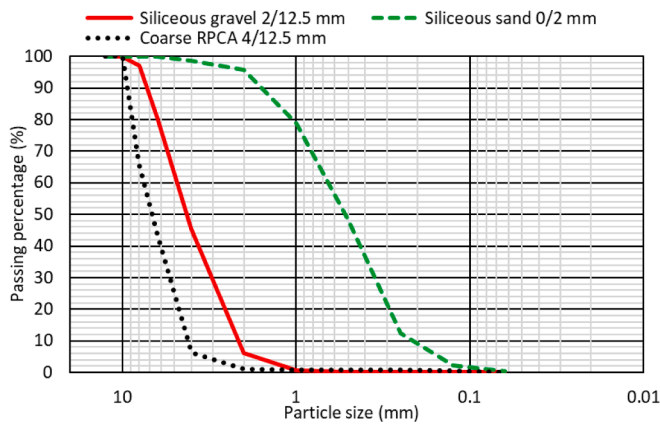


Fig. 1. Aggregate particle gradation.

Table 1

Density and water absorption of the aggregates as per EN 1097-6 [42].

Aggregate	Saturated-surface-dry density (Mg/m <sup>3</sup> )	24-hour water absorption (% wt.)
Siliceous sand 0/2 mm	2.63	0.26
Siliceous gravel 2/12.5 mm	2.61	1.16
Coarse RPCA 4/12.5 mm	2.41	4.15

- On the one hand, the water content was not changed when coarse RPCA was added. Thus, the higher water absorption of this sustainable aggregate compared to siliceous gravel (Table 1) led to a decrease in the effective water-to-cement ratio of the SCC [22,44]. The required compressive strength was therefore maintained when RPCA was added, although flowability decreased [45], reduction that was partly compensated for by increasing the amount of admixture.
- On the other hand, the requirement to limit the study to the coarse RPCA (larger than 4 mm) and the NA that were available at the precast-concrete plant meant that the siliceous gravel 2/12.5 mm was replaced by the larger-sized coarse RPCA 4/12.5 mm. To adjust the content of aggregate particles between 2 mm and 4 mm in size, the content of siliceous sand 0/2 mm was increased with the addition of coarse RPCA, as this natural sand also had particles of this size, as shown in Fig. 1.

The mixes were labelled either “HR-30” or “HR-45”, depending on the minimum compressive strength that was required. The label name was followed by the percentage of coarse RPCA (0 %, 20 %, 50 % and 100 %) incorporated in the mix. The composition of all mixes, which reflects the above aspects, is shown in Table 2.

Table 2

SSC mix design (kg/m<sup>3</sup>).

Mix	Cement	Water	Admixture 1	Admixture 2	Limestone filler	Siliceous sand	Siliceous gravel # Coarse RPCA
HR-30-0	250	112	0.50	1.30	320	650	1150 # 0
HR-30-20 %	250	112	0.50	1.30	320	650	920 # 250
HR-30-50 %	250	112	0.65	1.60	320	670	540 # 540
HR-30-100 %	250	112	0.85	2.00	320	720	0 # 1040
HR-45-0	320	112	0.50	1.30	280	650	1150 # 0
HR-45-20 %	320	112	0.50	1.30	280	650	920 # 250
HR-45-50 %	320	112	0.65	1.60	280	670	540 # 540
HR-45-100 %	320	112	0.85	2.00	280	720	0 # 1040

### 2.3. Experimental plan

After mixing, the slump-flow test was performed according to EN 12350-8 [42]. Three sets of specimens were prepared and stored in a humid chamber (humidity  $95 \pm 5$  % and temperature  $20 \pm 2$  °C) until the test age: 15x30-cm<sup>3</sup> cylindrical specimens, 10x10x40-cm<sup>3</sup> prismatic specimens, and 10x10x10-cm<sup>3</sup> cubic specimens. The cylindrical and prismatic specimens were used to measure the compressive strength, modulus of elasticity, splitting tensile strength, and flexural strength at 28 days according to EN 12390-3, EN 12390-13, EN 12390-6, and EN 12390-5, respectively [42]. Cubic specimens were used for durability tests in marine environments. Each final result represented the arithmetic mean of the test results on three different specimens.

The durability tests within a marine environment, temporally distributed according to the flowchart in Fig. 2, are listed below. The procedure used in each test is detailed at the beginning of the section in which the results of each test are presented.

- As the durability behavior of concrete is closely linked to porosity [39], the capillary-water-absorption test, according to UNE 83966 [46] and UNE 83982 [47], provided an estimate of the porosity of the different mixes for comparative purposes [36]. In addition, the effect of the RPCA on the water absorption of SCC was also evaluated with the same test results [48]. The capillary-water-absorption test was performed at 28 and 180 days to evaluate the development of mix porosity.
- The formation of carbonates within concrete, which can corrode the reinforcement [37], is favored in environments with high relative humidity [30]. To evaluate this aspect, the mixes were subjected to a natural-carbonation test in an outdoor environment with high relative humidity, which began at an age of 28 days and lasted for one year. An accelerated-carbonation test was also performed at an age of 28 days according to EN 13295 [42], in which the carbonation depth and the Ultrasonic Pulse Velocity (UPV) variations as per EN 12505-4 [42] were evaluated.
- It is common to find industrial port buildings with an SO<sub>2</sub>-rich atmosphere [40]. A Kesternich test was conducted at 28 days in accordance with EN ISO 6988 [42], to evaluate the effect of this chemical compound on SCC with RPCA. In this test, the change in weight during the test and the variation of the UPV and compressive strength were assessed.
- Finally, three moist/dry tests were performed, each one in a different medium (drinking water, marine water, and sulfate water) to simulate the effect of tides [49]. The implementation of these tests was facilitated by personnel at the precast-concrete company, where moist/dry tests had on other occasions been performed under very demanding conditions. The three tests were performed one after the other, as all three could not be simultaneously performed, due to insufficient laboratory equipment and logistics problems. So, the drinking-water moist/dry test was initiated at 28 days, then the marine-water moist/dry test was performed, followed by the sulfate-water moist/dry test, as shown in Fig. 2. No specific criteria were followed to establish this order. During all three tests, variations in

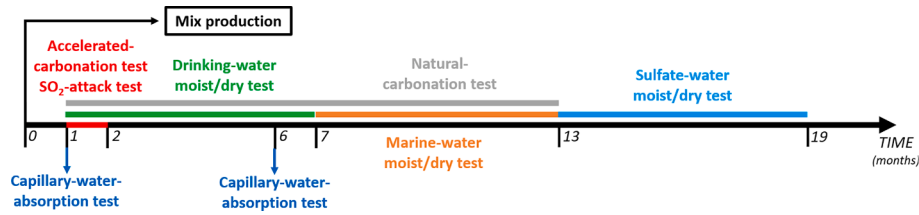


Fig. 2. Experimental plan for durability performance in marine environments.

weight, UPV readings, and compressive strength were successively noted and measured.

Finally, it is important to note that the compressive strengths recorded after the durability tests were compared with the strengths of non-durability-tested specimens. These non-durability-tested specimens were kept in a humid chamber and their compressive strengths were measured immediately after each durability test had ended, at exactly the same time and age as the specimens used in each durability test.

## 2.4. Models for service-life prediction through a carbonation approach

Based on the carbonation depth obtained in the accelerated-carbonation test, the expected service life was calculated for each mix according to four different models. In this way, the service lives of the SCC with RPCA and an SCC exclusively containing NA could be compared. A concrete cover of 20 mm, considered standard practice in reinforced-concrete structures [50], was applied.

### 2.4.1. Fick's model

Fick's model [51] establishes that the carbonated concrete depth responds to Eq. (1), in which  $d$  is the carbonated depth in mm;  $t$ , the time it takes to reach that carbonation depth in years; and  $K$ , a constant in  $\text{mm/year}^{0.5}$  that depends on the  $\text{CO}_2$  diffusion coefficient, and the environmental conditions ( $\text{CO}_2$  concentration).

$$d = K \times \sqrt{t} \quad (1)$$

The carbonation depth noted in the accelerated-carbonation test can be applied to calculate the constant  $K$  for the ambient  $\text{CO}_2$  concentration of that test, which is 20 %. The value of the constant can therefore yield an estimate of the time that the carbonation process might need to reach a depth of 20 mm (concrete cover) at a  $\text{CO}_2$  concentration of 20 %. With this time, and assuming a linear relationship between the carbonation time and the square root of the  $\text{CO}_2$  concentration [52], the time within which a carbonation depth of 20 mm may be reached under ambient conditions ( $\text{CO}_2$  concentration of 0.035 %) can be calculated, as shown in Eq. (2) (carbonation time at a  $\text{CO}_2$  concentration of 20 % being  $t_{20\%}$ , and the service life of the structure being  $t_{0.035\%}$ ).

$$\frac{t_{20\%}}{t_{0.035\%}} = \sqrt{\frac{20\%}{0.035\%}} \quad (2)$$

### 2.4.2. Structural-code model

The Spanish standard Structural Code contains a model for predicting the service life of a structure through carbonation without using experimental data [53]. This model is similar to Eq. (3), in which  $d$  is the assumed carbonation depth in mm;  $t$ , the time in years required to reach that carbonation depth under ambient conditions; and  $K_c$  is a carbonation coefficient. The carbonation coefficient,  $K_c$ , is calculated according to Eq. (4), in which  $C_{env}$  is an ambient coefficient that depends on whether or not the structure is protected from rain;  $C_{air}$  is an aeration coefficient whose value depends on the occluded air within the concrete;  $CS$  is the medium compressive strength of concrete in MPa; and  $a$  and  $b$  are coefficients that depend on the type of cement that is used. Considering a carbonation depth,  $d$ , of 20 mm in the calculations and

obtaining the coefficients indicated as *per* Structural Code tables, the calculated time,  $t$ , will be the service life of the structure.

$$t = \left( \frac{d}{K_c} \right)^2 \quad (3)$$

$$K_c = C_{env} \times C_{air} \times a \times CS^b \quad (4)$$

### 2.4.3. Papadakis' model

Papadakis *et al.* proposed a simplified model for calculating the carbonation depth in cement-lime mortar coatings in the early 1990s [54,55]. Since then, its use has become widespread and has been extended to a wide variety of cement-based materials, such as concrete [56]. This model corresponds to Eq. (5), where  $d$  is the carbonation depth in mm;  $t$ , the time in years required to reach that carbonation depth;  $RH$ , the percentage relative humidity;  $\gamma$ , the ambient  $\text{CO}_2$  concentration considered by volume;  $\rho_c$ ,  $\rho_w$ , and  $\rho_a$ , the densities of cement, water, and aggregates in  $\text{Mg/m}^3$ , respectively; and  $w/c$  and  $a/c$ , the water-to-cement and the aggregate-to-cement dimensionless ratios of concrete. The service life of each mix will be obtained by clearing the time,  $t$ , from Eq. (5), considering a carbonation depth of 20 mm.

$$d = 350 \times \frac{\rho_c}{\rho_w} \times \frac{w/c - 0.3}{1 + \frac{\rho_c}{\rho_w} \times w/c} \times \left( 1 - \frac{RH}{100} \right) \times \left[ \left( 1 + \frac{\rho_c}{\rho_w} \times w/c + \frac{\rho_c}{\rho_a} \times a/c \right) \times \gamma \times t \right]^{1/2} \quad (5)$$

### 2.4.4. Parrot's model

Unlike the structural-code and Papadakis' models, Parrot's model does not estimate the service life of a concrete structure as a function of a carbonation coefficient, but of the air permeability of the concrete [57]. Shown in Equation (6), the model has the following terms:  $d$  is the carbonation depth in mm;  $t$ , the time in years required to reach that carbonation depth;  $c$ , the content of alkali material in the concrete in kg CaO per  $\text{m}^3$ ; and  $K$ , is a constant equal to  $10^{-16}$  that reflects the air permeability of concrete. The service life of the structure is obtained by clearing the time,  $t$ , for a 20-mm concrete cover from Equation (6).

$$d = 64 \times \frac{K^{0.4} \times t^{0.5}}{c^{0.5}} \quad (6)$$

## 3. Results and discussion

### 3.1. Fresh and mechanical performance

The results of the slump-flow test as well as the mechanical properties are detailed in Table 3. It can be noted from a general approach that, in principle, all the mixes met the necessary requirements for use as structural concrete [50]. A detailed analysis of these properties can be found elsewhere [22].

In relation to the fresh behavior, the HR-30 mixes presented an SF1 slump-flow class (slump flow of  $600 \pm 50$  mm), while the slump-flow class in the HR-45 mixes was SF2 (slump flow of  $700 \pm 50$  mm), as *per* EFNARC [43]. This increased flowability in the HR-45 mixes was due to their higher cement content, added for increased strength (Table 2), which resulted in a higher proportion of cement paste in the fresh



**Table 3**  
Fresh and mechanical properties of SCC mixes.

Mix	Slump flow (mm)	$t_{500}$ (s)	Compressive strength (MPa)	Modulus of elasticity (GPa)	Splitting tensile strength (MPa)	Flexural strength (MPa)
HR-30-0	680	4	49.1	37.0	5.2	6.2
HR-30-20 %	600	5	50.0	38.5	5.1	6.3
HR-30-50 %	580	5	55.6	35.2	4.9	6.4
HR-30-100 %	550	7	56.8	34.0	4.9	5.6
HR-45-0	750	3	63.4	40.8	5.3	8.0
HR-45-20 %	710	3	64.1	42.6	5.2	7.8
HR-45-50 %	600	4	66.8	38.0	5.0	7.9
HR-45-100 %	650	7	72.8	37.8	5.0	7.8

concrete that favored SCC flowability [36]. As expected, and even more since the higher water absorption of RPCA was not compensated for in the mix design [24], the addition of this aggregate led to a reduction in slump flow. The increase in admixture content was sufficient to maintain adequate slump-flow levels, with the exception of mix *HR-30-100 %*, in which the slump flow was the minimum required value [43]. In relation to viscosity ( $t_{500}$ ), the effects of the increase in cement content and the addition of RPCA were the same, with all mixes presenting a VS2 slump-flow-viscosity class ( $t_{500}$  greater than 2 s), as per EFNARC [43].

Concerning mechanical performance, the first aspect to highlight is the ample safety margin of the compressive strength of the mixes produced at the precast-concrete plant, as both control mixes presented compressive strengths that were higher than the required ones (30 MPa and 45 MPa, respectively). The non-compensation of the high water absorption of RPCA and the high quality of the aggregate meant that its addition in no way worsened the mechanical behavior, as previously noted in the literature [58–60]. All properties remained more or less constant except for compressive strength, which even increased by about 15 % with the addition of 100 % coarse RPCA. This behavior confirmed that SCC design with coarse RPCA is a feasible option to produce concretes that are comparable to SCC with 100 % NA in terms of both in-fresh and mechanical behavior.

### 3.2. Capillarity water absorption

Water absorption by capillarity was measured at 28 and 180 days in accordance with the “Fangerlund method” described in Spanish standard UNE 83982 [47]. For this purpose, the specimens were previously conditioned in terms of humidity, in accordance with standard UNE 83966 [46], by keeping them in a humid chamber until two days before the test, at which time they were exposed to the laboratory environment. On the second of these two days, the skin on the lower face of the cubic specimens was removed and the lateral faces were waterproofed to prevent evaporation of the water within the specimens. After these two days, the specimens were placed in a tray with a grid, which was filled with water until 2 mm of the specimens were covered by water. The specimens were periodically weighed and kept under these conditions until the weight of all of them stabilized, which took approximately 23 days. The evolution of the weight increase per unit area for all the mixes at both test ages is detailed in Fig. 3, while Table 4 details the characteristic parameters of the capillarity-water-absorption behavior of the mixes.

The increase in the cement content led to a decrease of 0.5 units in absolute terms of the effective porosity  $\varepsilon_e$  (Table 4) at both 28 days and 180 days, which comprises the pores that are interconnected with each other. Thus, the *HR-45* mixes absorbed lower amounts of water (Fig. 3, and mass increase  $\Delta g$ , Table 4), although in all cases the temporal evolution of specimen weight was logarithmic due to the higher water

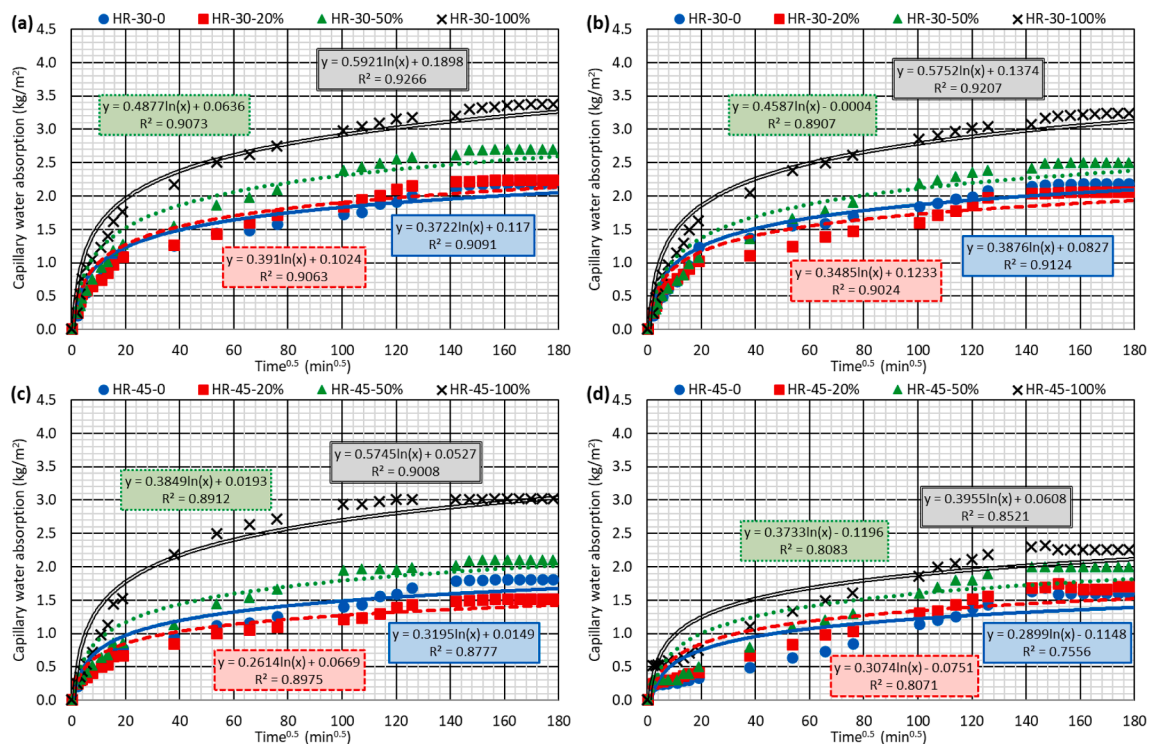


**Fig. 3.** Capillarity water absorption of SCC mixes: (a) *HR-30* at 28 days; (b) *HR-30* at 180 days; (c) *HR-45* at 28 days; (d) *HR-45* at 180 days.

**Table 4**

Capillary-water-absorption results. In brackets the percentage variation of each coefficient from 28 to 180 days.

Mix	28 days				180 days			
	$m$ (min/cm <sup>2</sup> ) <sup>1</sup>	$\Delta$ (g) <sup>2</sup>	$\varepsilon_e$ (%) <sup>3</sup>	$K$ (g/m <sup>2</sup> min <sup>0.5</sup> ) <sup>4</sup>	$m$ (min/cm <sup>2</sup> ) <sup>1</sup>	$\Delta$ (g) <sup>2</sup>	$\varepsilon_e$ (%) <sup>3</sup>	$K$ (g/m <sup>2</sup> min <sup>0.5</sup> ) <sup>4</sup>
HR-30-0	460.82	38.7	2.92	13.60	460.82 (0.0)	38.7 (0.0)	2.92 (0.0)	13.60 (0.0)
HR-30-20 %	435.20	39.6	2.99	14.32	435.20 (0.0)	36.4 (−8.1)	2.75 (−8.0)	13.17 (−8.0)
HR-30-50 %	435.20	47.7	3.60	17.26	435.20 (0.0)	44.2 (−7.3)	3.33 (−7.5)	15.98 (−7.4)
HR-30-100 %	512.03	59.6	4.49	19.86	512.03 (0.0)	57.3 (−3.9)	4.32 (−3.8)	19.09 (−3.9)
HR-45-0	435.20	32.0	2.41	11.57	435.20 (0.0)	28.3 (−11.6)	2.13 (−11.6)	10.23 (−11.6)
HR-45-20 %	435.20	26.9	2.03	9.71	537.62 (+23.5)	30.2 (+12.3)	2.28 (+12.3)	9.83 (+1.2)
HR-45-50 %	435.20	37.3	2.81	13.49	358.42 (−17.6)	35.3 (−5.4)	2.67 (−5.0)	14.09 (+4.4)
HR-45-100 %	435.20	53.4	4.03	19.30	409.60 (−5.9)	39.9 (−25.3)	3.01 (−25.3)	14.89 (−22.8)

<sup>1</sup> Resistance to water penetration by capillarity.<sup>2</sup> Mass increase.<sup>3</sup> Effective porosity.<sup>4</sup> Capillarity-absorption coefficient.

absorption at the beginning of the test. It can therefore be appreciated that the higher the amount of hydration products from the increased cement content in the SCC, the more effective the expulsion of air during setting, resulting in lower porosity levels within the mixes [61]. This phenomenon partially explained the higher strength of concrete as the cement content was increased (Table 3), as it is clear that the lower the porosity levels, the better the mechanical behavior of concrete [36]. In addition to reduced porosity, the increase in cement content caused the interconnected pores to form more tortuous capillary networks, which slowed the rate of water penetration into the concrete. The effects are clearly evident in the capillarity-absorption coefficient,  $K$ , which was on average 3 units lower in the HR-45 mixes than in the HR-30 mixes, and the resistance to water penetration by capillarity,  $m$  (Table 4); both indicators of speed of entry of the water into the concrete [48].

The addition of coarse RPCA had the opposite effect of increasing the cement content, i.e., its addition augmented the amount of absorbed water, the effective porosity,  $\varepsilon_e$ , and the capillarity-absorption coefficient,  $K$ , regardless of the age of study. Furthermore, the fitting accuracy of the logarithmic model of the evolution of capillary water absorption as a function of time increased with the content of coarse RPCA due to the higher initial water absorption of the concrete mixes that incorporated this waste (Fig. 3). Therefore, the addition of coarse RPCA not only led to an increase in the porosity of the cementitious matrix, mainly due to the lower density of the ITZ that it generated, but it also caused an increase in the interconnected pores, creating a way for water to penetrate more easily and quickly into the SCC [60]. However, the addition of small amounts of coarse RPCA, such as 20 %, was not negative and even improved the capillary behavior of the SCC. It is important to note that the increase in porosity when using RPCA was small, as the maximum increase in effective porosity,  $\varepsilon_e$ , with 100 % coarse RPCA was, for example, 1.5 units, which was lower than in other studies cited in the bibliography [36,48]. This statement is also supported by the mechanical behavior of the mixtures (Table 3), as the properties of SCC remained almost constant despite the increase in porosity after adding RPCA.

No synergistic interaction was observed between the effects of the amount of cement and the content of coarse RPCA on the 28-day effective porosity,  $\varepsilon_e$ , of the SCC. Therefore, the variation of the 28-day effective porosity with the addition of the different coarse RPCA contents was similar in both the HR-30 and the HR-45 mixes. However, the increase in effective porosity at 180 days with increasing RPCA content in the HR-45 mixes was much lower than in the HR-30 mixes, which can be observed in Table 4 and Fig. 3. The same behavior was reflected in the capillarity-absorption coefficient  $K$  at both ages, i.e., the increase in this coefficient caused by the addition of coarse RPCA was lower in the HR-45 mixes than in the HR-30 mixes. It therefore appears that the hydration of larger amounts of cement results in higher density of the ITZ formed by RPCA, thus partly compensating the negative effect of this sustainable aggregate [61]. So, the SCC presented smaller and

more sinuous capillary networks for the entry of water [48], especially in the long term, when this behavior is observable both through the effective porosity and the capillarity-absorption coefficient.

Finally, if the temporal evolution of both the effective porosity,  $\varepsilon_e$ , and the capillarity-absorption coefficient,  $K$ , are analyzed, highly disparate results can be detected. However, it can in general terms be stated that, in accordance with Table 4, both the effective porosity,  $\varepsilon_e$ , and the capillarity-absorption coefficient,  $K$ , decreased from 28 days to 180 days in the HR-45 mixes, while the variations were much smaller in the HR-30 mixes. Thus, a higher cement content in the SCC appeared not only to lead to partial compensation of the damaging effect of coarse RPCA on the capillary behavior of SCC, as explained in the previous paragraph, but also to the fact this behavior will improve over time in any SCC mix, regardless of the type of aggregate in use.

### 3.3. Carbonation

#### 3.3.1. Natural carbonation

The natural-carbonation test was performed when the mixes had aged for 28 days. This test simply consisted of leaving the specimens in an outdoor environment (CO<sub>2</sub> concentration of 0.035 %) with high relative humidity and temperature changes for one year. Temperature and humidity were defined to be unfavorable for the concrete in carbonation terms [12], and were continuously recorded throughout the test, as shown in Fig. 4. Subsequently, the specimens were split in half and sprayed with phenolphthalein, leaving a pink-to-deep-red hue except in the carbonated zones where the indicator remained colorless.

No clear carbonate surface was observed in any of the mixes, all of which showed a low-porosity skin that hindered CO<sub>2</sub> penetration within the concrete. As only the coarse fraction of RPCA was used in this study,

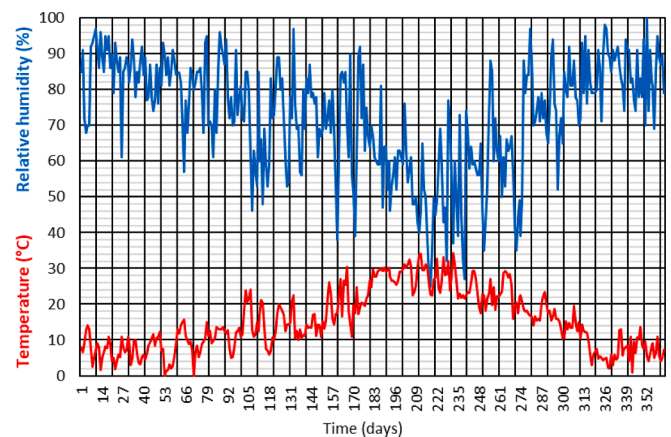


**Fig. 4.** Evolution of temperature and relative humidity during the natural carbonation test.

the skin was not affected by the use of this aggregate, as opposed to what could have happened if fine RPCA had been used [62]. Thus, the skin effect remained the same despite the addition of coarse RPCA. To exemplify this idea, specimens for all the mixes *HR-45* after this test are shown in Fig. 5. However, it should be noted that carbonated zones were found in some mixes, such as in the *HR-45-20* % mix, due to the existence of local defects on the concrete skin, which underlines the importance of an adequate surface finish of the concrete to avoid this sort of result [63].

### 3.3.2. Accelerated carbonation

The accelerated-carbonation test was performed to evaluate the effect of the coarse RPCA once  $\text{CO}_2$  had penetrated within the SCC, passing through the carbonation barrier on the surface due to the concrete skin. To do so, 28-day-old specimens were placed in an accelerated-carbonation chamber for 4 weeks, following the requirements of EN 13295 [42]. In this test,  $\text{CO}_2$  reacts with calcium hydroxide in a high humidity environment, as it progressively penetrates the concrete, leading to the formation of calcium carbonate [51]. Following EN 12505-4 [42], after the exposure period, the UPV was measured on the carbonated specimens and compared with the UPV measures conducted before the test. Then, the carbonated specimens were split in half and the surfaces were sprayed with phenolphthalein to evaluate their carbonation. As  $\text{CO}_2$  penetrated into all the specimens in the accelerated-carbonation test, a clearly carbonated (colorless) surface appeared on all of them, as shown in Fig. 6. The average carbonation depth was measured on each of these carbonated surfaces.

The carbonation depth (Fig. 7a) showed a behavior similar to that observed in the capillary-water-absorption test, as higher SCC porosity led to easier and deeper  $\text{CO}_2$  penetration [12]. Thus, the *HR-45* mixes, with a higher cement content, showed carbonation depths that were between 0.2 and 0.5 mm lower than the *HR-30* mixes for coarse RPCA contents between 0 % and 50 %, although this decrease was around 1 mm when 100 % coarse RPCA was employed. The higher amount of cement in the mix design of the *HR-45* mixes led to a higher proportion of cementitious matrix when hardened, which in turn resulted in a lower number of pores that were also less interconnected with each other, which hindered  $\text{CO}_2$  penetration [40]. In addition, in the *HR-45* mixes the ITZ density levels were not as low after RPCA additions [61], which was reflected in the higher decrease in the carbonation depth with higher amounts of coarse RPCA.

Fig. 7a details effects of coarse RPCA on the carbonation depth. As with other studies in which the carbonation behavior of recycled aggregate concrete has been analyzed [24,62], increasing proportions of this sustainable aggregate also increased the carbonation depth. In this case, the carbonation depths were between 3 mm and 4 mm for 0 % coarse RPCA and between 4.5 mm and 6 mm for 100 % coarse RPCA.

The increases were due to the increased porosity of the cementitious matrix, especially in the ITZ, following the addition of this aggregate [36]. On the other hand, the higher porosity of coarse RPCA compared to coarse NA, due to the presence of adhered mortar, also affected this performance [33], as shown in Fig. 8 for the *HR-45-100* % mix. Thus, it was noted that some RPCA particles in the external area of the SCC specimens remained colorless once they had been sprayed with phenolphthalein (carbonated particles of RPCA), which led to an increase in the carbonation depth. This behavior of RPCA also allows its carbonation treatment to improve its performance when used in concrete production [30]. However, the addition of small amounts of coarse RPCA, such as 20 %, had no negative effect. In addition, the carbonation depth was low, with mean values below 6 mm in all cases, below the required minimum concrete cover of 20–25 mm in the reinforced-concrete design standards [50].

Finally, the UPV results are detailed in Fig. 7b. As the UPV increased in all mixes after the accelerated-carbonation test, it can be stated that the strength of the mixes increased as a result of carbonation, due to higher strengths within the surface zone resulting from the presence of calcium carbonate [30]. In addition, the higher in UPV test results, the higher the content of coarse RPCA. Carbonation is known as one of the best treatments for improving the performance of recycled aggregate, adding greater hardness and strength to the adhered mortar [64]. Therefore, the particles of coarse RPCA within the SCC were carbonated during the accelerated-carbonation test, as shown in Fig. 8, which improved their performance and caused the UPV of SCC to decrease, indicating an increase in compressive strength [65].

### 3.3.3. Service-life prediction through carbonation

The service life of structures (20-mm concrete cover) made with the SCC mixes under study was predicted on the basis of carbonation through the models shown in Section 2.4. The following aspects were considered:

- Fick's model (Eq. (1) and Eq. (2)) was applied according to the results of the accelerated-carbonation test. It can be considered the most accurate model, since it is based on experimental results [56].
- The structural-code model (Eq. (3) and Eq. (4)) was applied, considering the most unfavorable values of the coefficients  $C_{env}$  (SCC exposed to rain) and  $C_{air}$  (air content of SCC higher than 4.5 %) [53]. Coefficients  $a$  and  $b$  were those corresponding to CEM I. The value of the medium compressive strength for each mix is shown in Table 3.
- A cement density of  $3.12 \text{ Mg/m}^3$ , an average NA density of  $2.60 \text{ Mg/m}^3$  (Table 1), an average RPCA density of  $2.41 \text{ Mg/m}^3$  (Table 1), a  $\text{CO}_2$  concentration of 0.035 %, and a relative humidity of 60 % were considered in Papadakis' model (Eq. (5)). The water-to-cement and

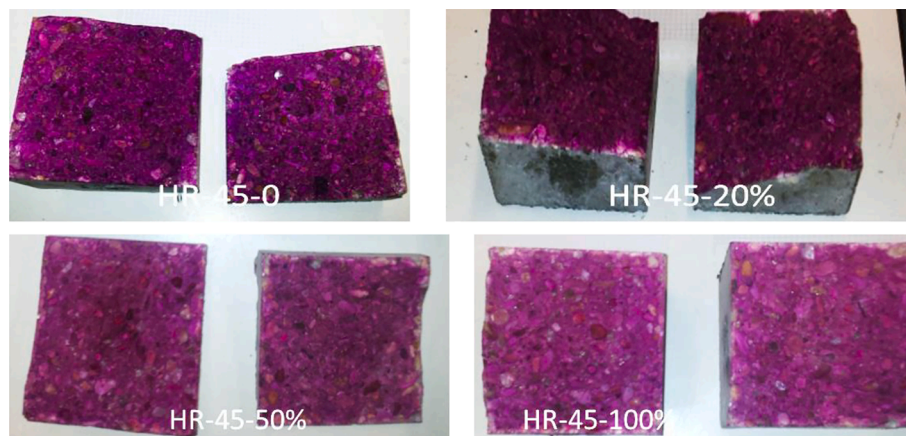


Fig. 5. Specimens of *HR-45* mixes sprayed with phenolphthalein after the natural-carbonation test. The uncolored area is the carbonated area in each specimen.



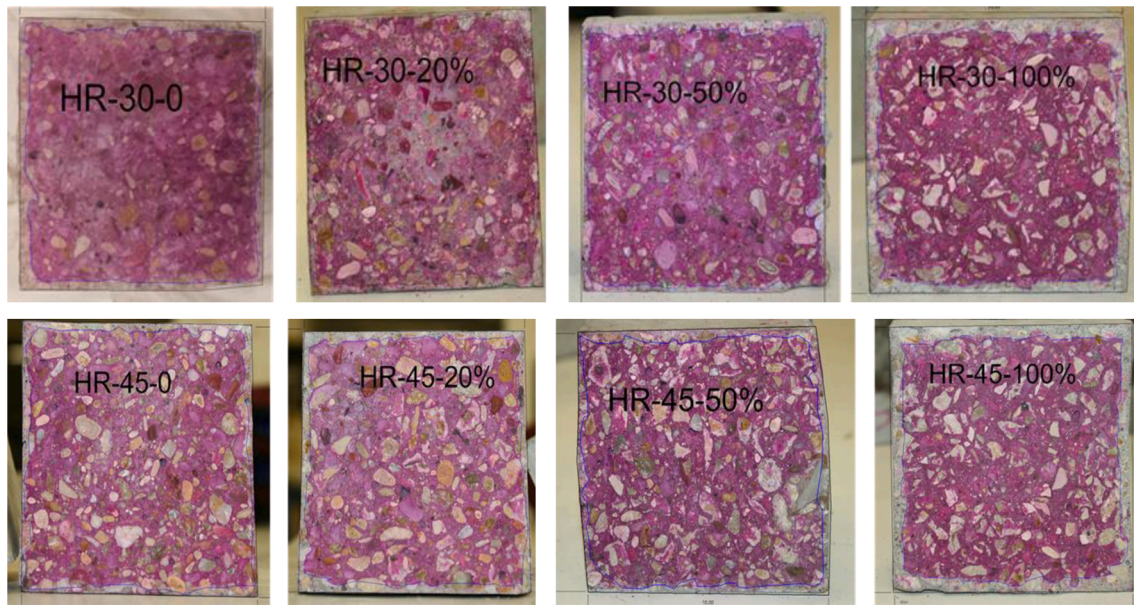


Fig. 6. Specimens sprayed with phenolphthalein after accelerated-carbonation test. The uncolored area is the carbonated area in each specimen.

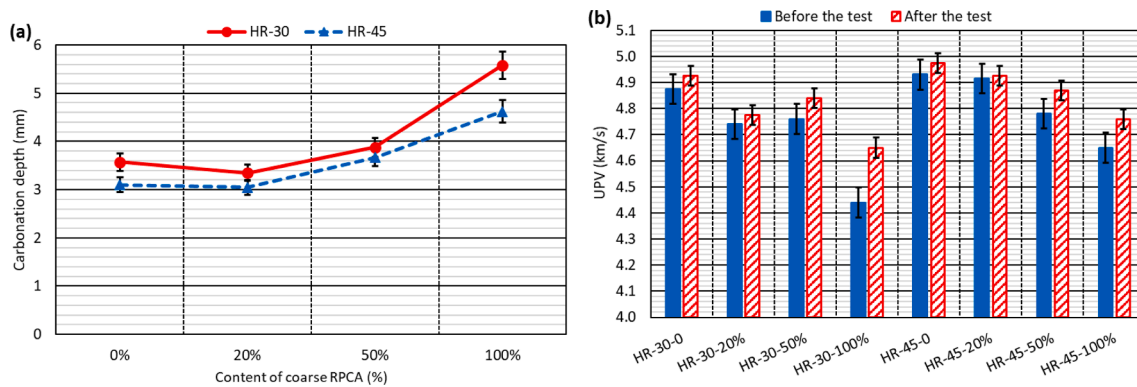


Fig. 7. Accelerated-carbonation tests: (a) carbonation depth; (b) UPV results.

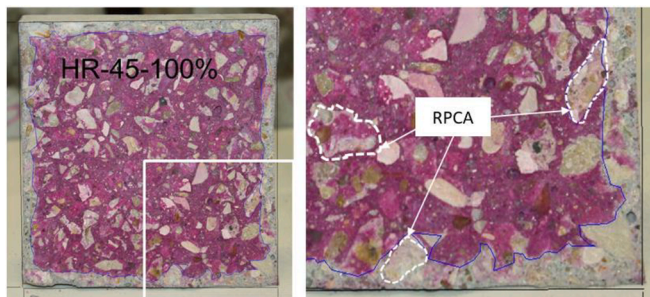


Fig. 8. Carbonation permeability of adhered mortar in a specimen of the HR-45-100% mix.

cement-to-aggregate ratios were calculated in accordance with the mix compositions (Table 2).

- Finally, Parrot's model (Eq. (6)) was applied considering that the amount of CaO in the cement indicated by the manufacturer was 63.9 % by weight.

Fig. 9 shows the service life calculated from each model. Fick's model showed a service life for all mixes of around 100 years, the maximum required by the structural design regulations [50]. As expected from the

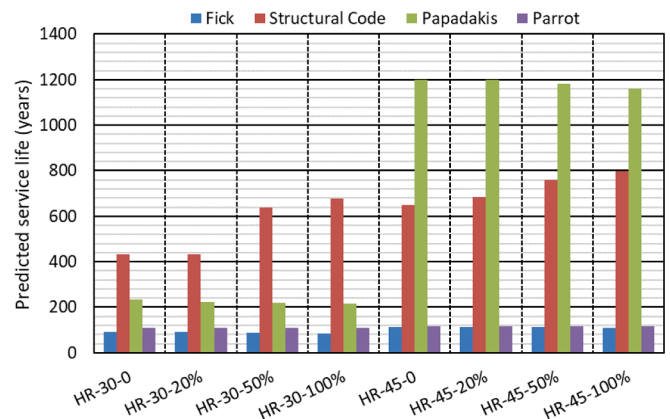


Fig. 9. Predicted service life based on carbonation.

accelerated-carbonation results, the service life lengthened as the cement content increased and the RPCA content remained low, although the differences between the mixes with 0 % and 100 % coarse RPCA were less than 10 years. Parrot's model was the theoretical model that best matched Fick's model, with service life values also around 100 years. Both the structural-code model and Papadakis' model clearly



overestimated the service life of SCC. For example, the structural-code model overestimated the service life of all the mixes, reporting service lives between 400 and 800 years. Although it reported a longer service life for the HR-45 mixes, it predicted longer service lives with higher RPCA contents, due to the increase in compressive strength after adding coarse RPCA (Table 3). Nevertheless, this trend did not fit with the results obtained in the accelerated-carbonation test. Papadakis' model properly predicted the effect of increased cement content and the addition of coarse RPCA. However, although the overestimation of service life was small for the HR-30 mixes (service life around 200 years), the overestimation was very high for the HR-45 mixes, due to their low water-to-cement ratio (service lives of around 1200 years). On this basis, it can be stated that the Papadakis' model is valid for conventional water-to-cement ratios.

### 3.4. SO<sub>2</sub> attack

The SO<sub>2</sub>-attack test or Kesternich test is commonly used to evaluate the corrosion of metals. However, it has been found that in an SO<sub>2</sub>-rich environment, ettringite and thaumasite can form in the cementitious matrix of concrete, which can affect its strength behavior [66]. As there may be industrial port buildings with an SO<sub>2</sub>-rich atmosphere, it was considered that the performance of this test was convenient. Following EN ISO 6988 [42], the SCC specimens were subjected to 15 cycles of 24 h. Each cycle consisted of two stages. In the first stage, the specimens were exposed for 8 h to SO<sub>2</sub>-saturated water vapor (humidity of 100 %) at  $40 \pm 2$  °C. The second stage consisted of exposing the specimens to the laboratory environment for 16 h for air-cooling at  $20 \pm 2$  °C. After completion of the cycles, the variation in weight, UPV readings, and compressive strength were evaluated, the results of which are shown in Fig. 10.

As expected, the weight of the mixes had increased after the test (Fig. 10a), due to the formation of the aforementioned compounds. The weight increase was undoubtedly linked to the porosity of the mixes (Table 4), since a higher effective porosity led to a higher penetration of SO<sub>2</sub> within the SCC and to the formation of higher amounts of ettringite

and thaumasite [67]. Thus, the addition of coarse RPCA led to an increase in SCC porosity, which in turn led to higher weight gains. This trend was observed mainly in the HR-30 mixes, since they were the most porous, while the HR-45 mixes, whose increase in porosity when RPCA was added was lower, due to the higher cement content, presented trends that were more random in relation to their weight variation.

Both the UPV (Fig. 10b) and the compressive-strength results (Fig. 10c) showed that exposure to large amounts of SO<sub>2</sub> was not negative for the mixes, as the UPV readings and, consequently, the compressive strength increased after the test. In studies on concretes produced with CEM III, it was found that the compressive strength decreased after this test [40]. In this case, CEM I was used, so a cementitious matrix of higher quality and mechanical strength was obtained, which might explain why the strength increased rather than decreased and why the strength increase was greater when larger cement amounts were added. No clear trend, either positive or negative, can be established from these test results, in relation to the strength behavior of SCC containing varying amounts of coarse RPCA. It can therefore be stated that the use of RPCA has little or no effect on the mechanical behavior of SCC in a SO<sub>2</sub>-rich environment.

### 3.5. Moist/dry processes

Three moist/dry tests were performed in different media (drinking water, marine water, and sulfate water) in succession, as there was insufficient laboratory equipment to perform the tests simultaneously (Fig. 2). The three moist/dry tests were performed following the same procedure, which was defined at the precast-concrete company, based on previous tests it had performed for the design of some of its concretes. First, the specimens were oven dried for 2 days, after which time they were weighed (initial weight) and their UPV was measured. Subsequently, they were subjected to 27 moist/dry cycles, which consisted of immersion for 5 days in the test medium at  $20 \pm 2$  °C and oven drying at  $70 \pm 2$  °C for 2 days, temperatures defined as *per* ASTM D 559 [68]. After every 3 cycles, the specimens were weighed. At the end of the test, the specimens underwent UPV and compressive-strength testing. At the

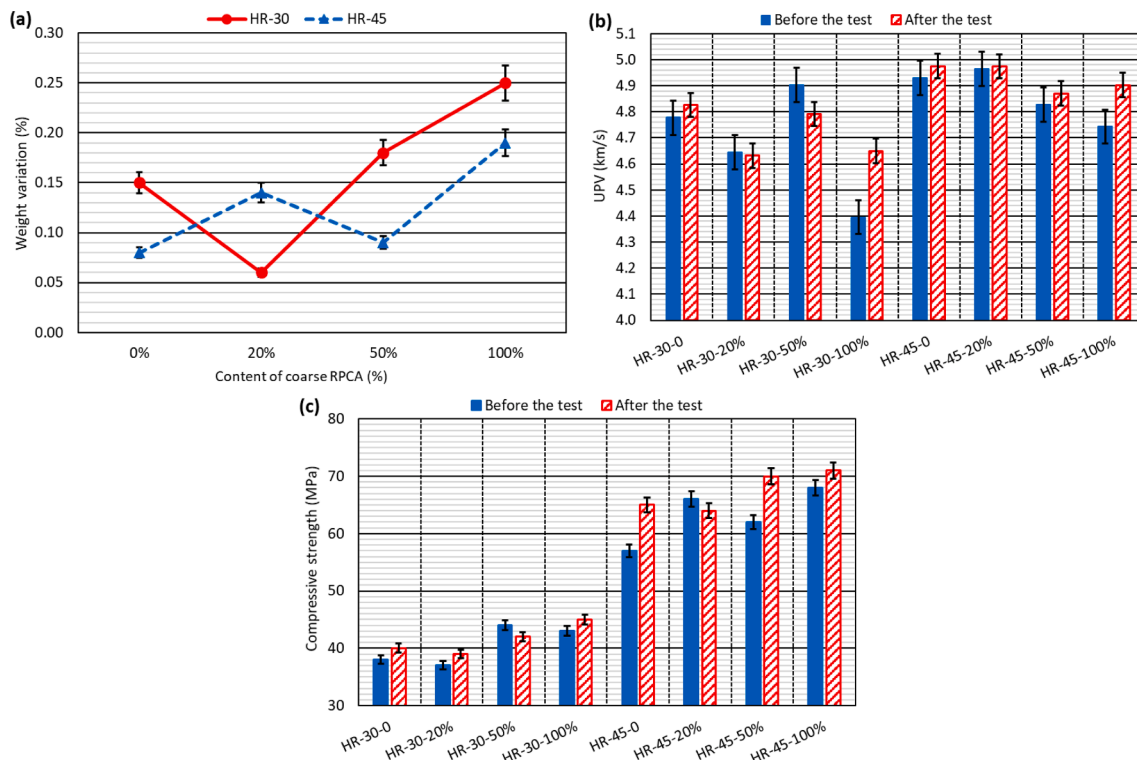


Fig. 10. SO<sub>2</sub>-attack test: (a) weight variation; (b) UPV results; (c) compressive-strength results.

same time, the compressive strength of specimens of the same age, which had been kept in a humid chamber rather than undergo moist/dry tests, was measured. In this way, the evolution of the weight throughout the test and the effect of the moist/dry cycles on the UPV and compressive strength of the SCC were all assessed.

### 3.5.1. Drinking water

The changes in the weight of the specimens, which always increased in a continuous way throughout the drinking-water moist/dry test, are detailed in Fig. 11a. Since the specimens were oven-dried prior to the test, the same way as when weighed during the test cycles, this weight increase could not be primarily attributed to water absorption within the SCC. It was therefore presumed that the weight increase was due to delayed hydration of the cement, which led to hardening and clogging of some pores and, in turn, to a higher weight of the SCC [40]. The same conclusion is supported by the behavior of the HR-30 and HR-45 mixes, as the weight variation was either equal or slightly higher in the mixes with higher cement content for the same amount of coarse RPCA (greater difference by 0.05 % in absolute terms). Regarding coarse RPCA, it can be stated that there was no linear relationship between the content of this aggregate and the weight increase, although the mixes with less coarse RPCA content (0 % and 20 %) underwent lower weight increases than the mixes with 50 % and 100 % coarse RPCA. The coarse RPCA presented adhered mortar, which can also undergo some slight hydration and might, therefore, have increased in weight during the test [69].

The UPV results (Fig. 11b) underwent a significant increase after the test, revealing the absence of internal damage in the concrete following thermal shock [37]. This observation was supported by the small increase in compressive strength that the SCC mixes mostly experienced (Fig. 11c), which in turn supports the theory advocated in the previous paragraph concerning the delayed hydration of the cement, process favored by the low age of the specimens when the test started (28 days) and the long drying periods conducted. No clear trend of the effect of cement and coarse RPCA content was observed from the UPV readings,

which can be attributed to the variability of this measure [65]. However, it was noted that the increase in compressive strength was greater in mixes with higher cement and RPCA contents. A behavior that may be clearly explained because most of the new hydration products were generated in these mixes during the test, due to the higher cement content and the higher content of coarse RPCA with larger amounts of adhered mortar [69].

### 3.5.2. Marine water

The results of the marine-water moist/dry test are shown in Fig. 12. The presence of large amounts of chlorides in the chemical composition of marine water changed the weight of the SCC in non-linear patterns of increasing complexity (Fig. 12a). Three different stages could be distinguished in the weight evolution:

- During the first 9 cycles, an increase in specimen weight was observed, possibly due to the delayed hydration process of the cement [69], analogous to what was noted in the drinking-water moist/dry test.
- Between cycles 9 and 21, weight loss affected the mixes that all fell below their initial weights. The presence of large amounts of chlorides within the marine water led to the formation of chloroaluminates of lower molecular weight that could be leached out by the seawater [49].
- From cycle 21 to the end of the test, the specimens again increased in weight. There were perhaps very few unleached chloroaluminates in the specimens as from cycle 21 onwards, which may have led to the precipitation of the salts present in the seawater within the porous network of the concrete which outweighed the leaching process, causing a progressive increase in weight [70]. As a result of this final process, the specimens adopted a whitish surface color (Fig. 13).

If the mixes with the same coarse RPCA contents are compared, it can be appreciated that the weight variations described were greater in the HR-30 mixes. Unlike in the drinking-water moist/dry test, in which the

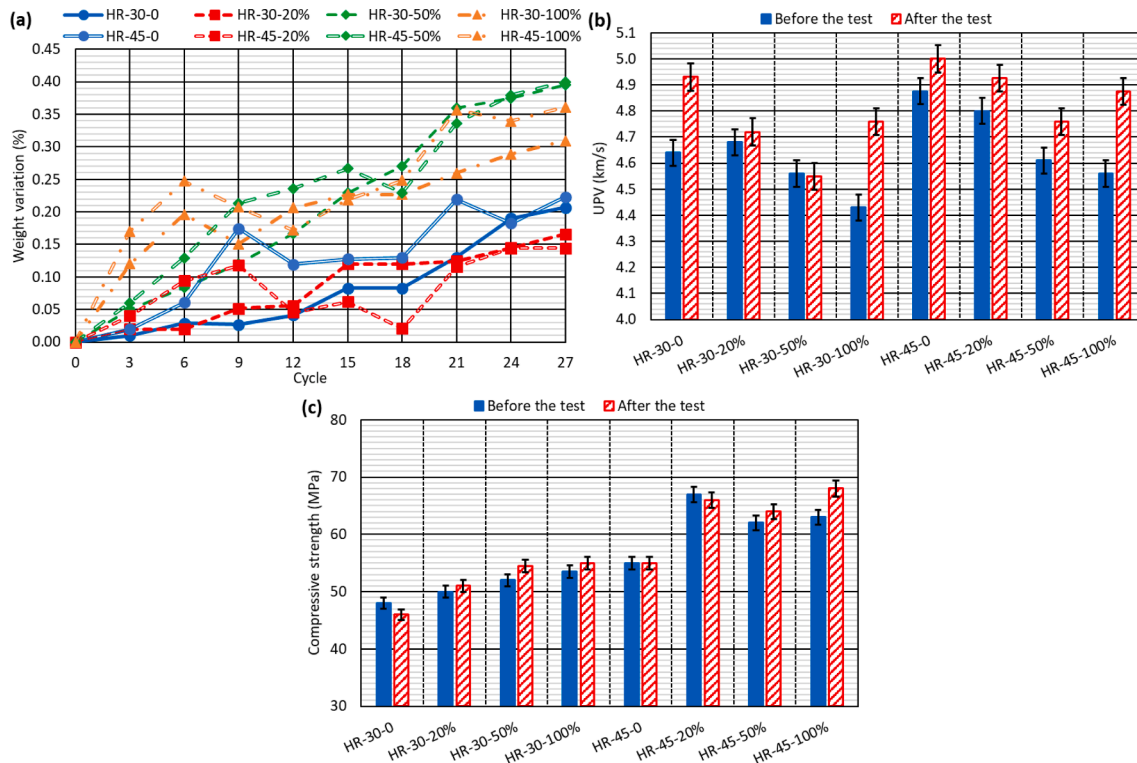


Fig. 11. Drinking-water moist/dry test: (a) weight variation; (b) UPV results; (c) compressive-strength results.

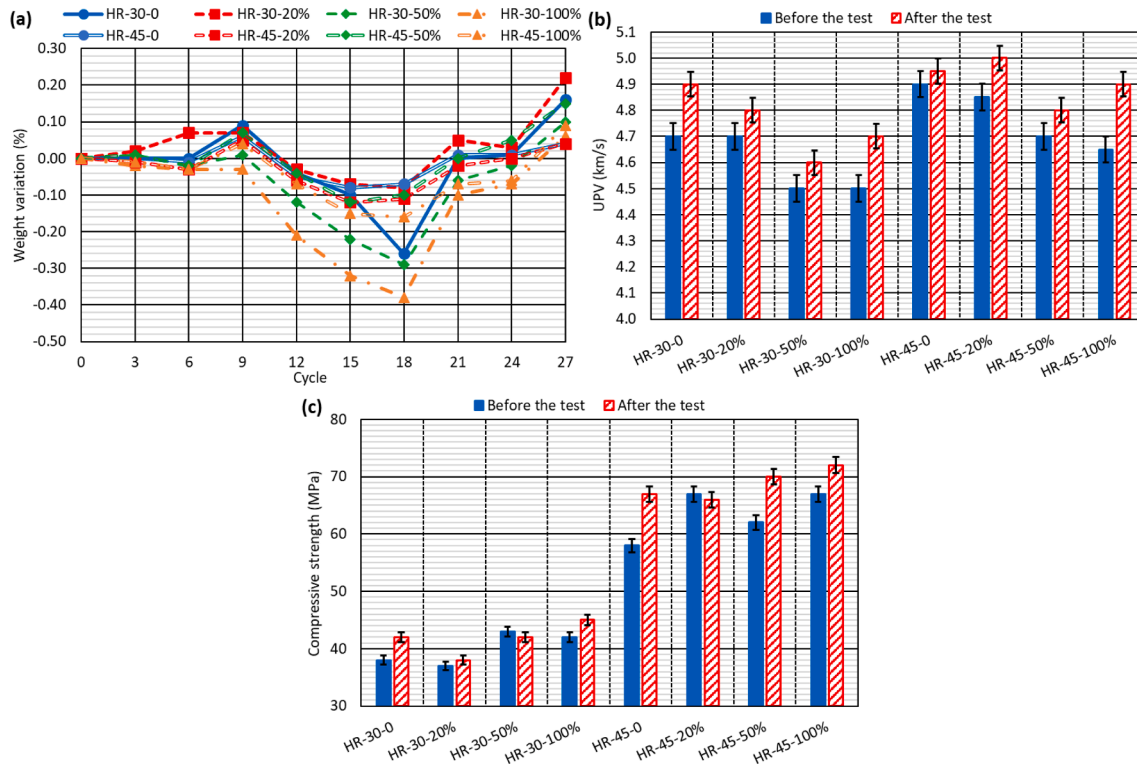


Fig. 12. Marine-water moist/dry test: (a) weight variation; (b) UPV results; (c) compressive-strength results.



Fig. 13. Appearance of specimens after completion of the marine-water moist/dry test.

increase in concrete weight depended basically on cement hydration, it is thought that porosity played a very important role in this chloride penetration within SCC [67]. The higher porosity of the HR-30 mixes (Table 4) meant that the aforementioned chemical processes could occur more easily. The effect of coarse RPCA was also linked to porosity, as the mixtures with low RPCA contents, which showed lower porosity (Table 4), presented a more constant weight.

Fig. 12b and Fig. 12c show the variation of UPV and compressive-strength results, respectively. As in the drinking-water moist/dry test, both magnitudes increased, as a result of cement hydration and pore clogging [69,70]. However, the relative increase in compressive strength was greater in this case in the control mixes (0 % coarse RPCA). An initial hypothesis might be that the strength increase was lower when using RPCA due to the higher crystallization of salts within the mixes that incorporated this aggregate.

### 3.5.3. Sulfate water

The sulfate water in which the specimens were immersed in this test

was prepared with distilled water with a 5 % concentration of potassium sulfate ( $K_2SO_4$ ). The test results are shown in Fig. 14. While the UPV and the compressive strength showed similar behaviors to the results of the marine-water moist/dry test, the changes in weight were different.

The weight of the specimens (Fig. 14a) continuously increased throughout the test, initially more markedly, they began to stabilize around cycle 15. These changes might mainly be due to the formation of ettringite or tricalcium sulfoaluminate, as a consequence of the reaction between the sulfate ion and the tricalcium aluminate resulting from the cement hydration [71]. Its higher molecular weight led to a progressive increase in weight, which was found to be between 0.40 % and 0.80 % at the end of the test. This process was porosity dependent [41], so that the higher porosity of the mixes with lower cement contents and higher coarse RPCA contents led to a more pronounced weight increase.

All the mixes had higher compressive strengths after the test (Fig. 14b), as was also evident from the UPV readings (Fig. 14b). This behavior was due to the clogging of the pores of the mix and the hydration of the cement during the test [39]. However, it can also be

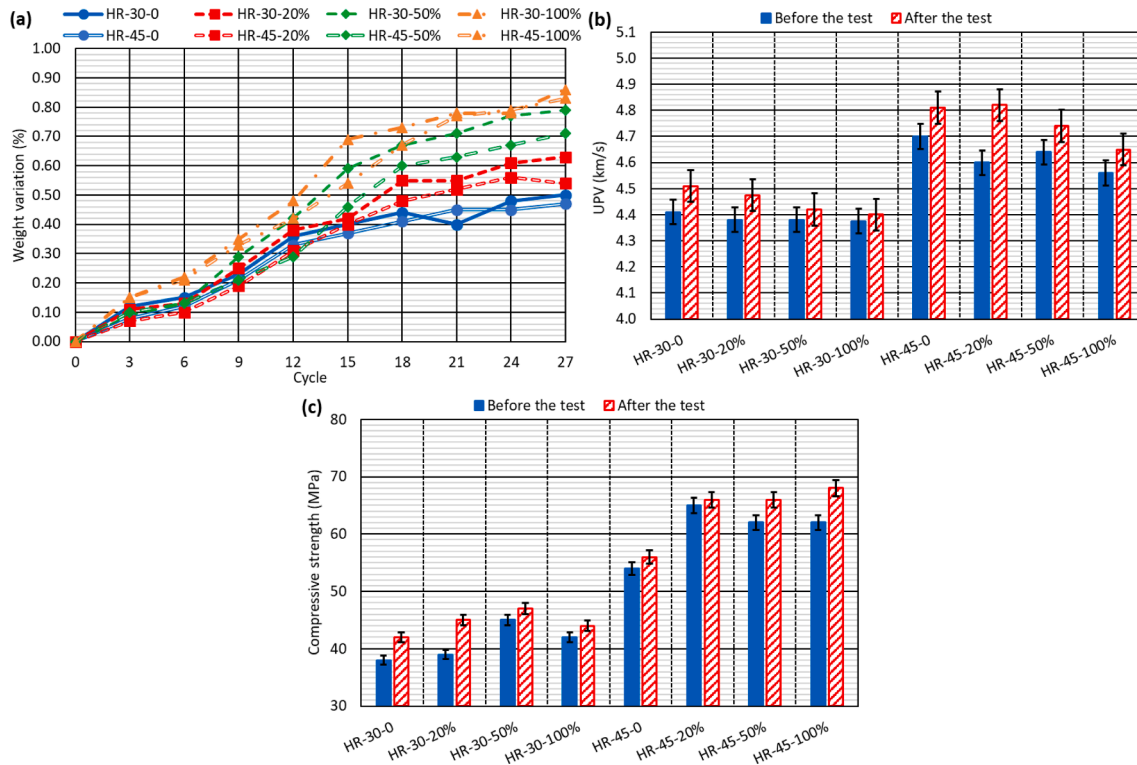


Fig. 14. Sulfate-water moist/dry test: (a) weight variation; (b) UPV results; (c) compressive-strength results.

observed that the increase in strength was greater in the mixes with high coarse RPCA contents, especially in the *HR-45* series. The formation of ettringite, which has a larger volume than the compounds from which it is formed, produces expansion within the concrete and the appearance of internal micro-cracking [63], which can be reduced with the addition of RPCA, due to its greater flexibility compared to NA [27].

#### 4. Conclusions

In this paper, the durability performance in a marine environment of Self-Compacting Concrete (SCC) made with 0 %, 20 %, 50 %, and 100 % coarse Recycled Precast-Concrete Aggregate (RPCA) has been analyzed. In addition, two different cement contents have been considered in the SCC to achieve different target compressive strengths. Capillary-water-absorption, natural-carbonation, accelerated-carbonation,  $\text{SO}_2$ -attack, drinking-water moist/dry, marine-water moist/dry, and sulfate-water moist/dry tests were all performed, in a simulation of a marine environment. The following conclusions have been drawn from the test results:

- Increasing the content of coarse RPCA led to a higher effective porosity and, therefore, to higher capillary water absorption levels. However, the addition of higher cement amounts lowered the increase in porosity resulting from the addition of RPCA. Furthermore, the temporal decrease in SCC porosity was greater when large amounts of RPCA were used. Thus, the expected increase in porosity when adding coarse RPCA can be partially compensated through a mix design with a slightly higher cement content, which is also reduced over time, a very relevant aspect in marine or submerged environments, where civil works are designed to have a long service life.
- Regardless of the mix design, the natural carbonation of the SCC over one year was negligible. The depth of carbonation under accelerated conditions was greater in mixes with low cement content and large amounts of coarse RPCA, i.e., in mixes with higher porosity.

However, RPCA carbonation during this test resulted in a strength increase according to the ultrasonic-pulse-velocity readings. All mixes reached a service life of at least 100 years according to calculations based on carbonation behavior.

- Exposure to a  $\text{SO}_2$ -rich environment caused a slight increase in weight, which was greater in the more porous SCC mixes. In addition, SCC also experienced an increase in compressive strength, although no clear trend could be discerned from the effect of the coarse RPCA. Thus, the use of SCC with large amounts of coarse RPCA would be appropriate in this type of industrial environments.
- Exposure to moist/dry cycles caused a variation in SCC weight, which was more pronounced at higher porosity levels, i.e., the lower the cement content the higher the coarse RPCA content. While drinking water and sulfate water increased the weight of the SCC, due to delayed cement hydration and ettringite formation, marine water initially caused a decrease in weight and then a subsequent increase. However, regardless of the medium and mix composition, the weight increases were slight, with maximum values of 0.80 %.
- The three moist/dry tests also yielded an increase in compressive strength in all mixes. The delayed hydration of the cement present in the adhered mortar of the coarse RPCA and its greater flexibility compared to the natural aggregate led to greater strength increases in drinking water and sulfate water, with even higher strength increases when the cement content was augmented. It is suspected that in marine water, the higher porosity of SCC containing RPCA, may have meant that any increase in strength was lower, due to salt deposition within the pores of the SCC.

In general terms, it can be affirmed that the use of RPCA has shown no adverse effects that might invalidate its use in SCC exposed to marine environment. It was even observed that the use of this aggregate improved some aspects, and that key improvements to its behavior can result from a precise definition of the cement content for any given construction purpose.



## CRediT authorship contribution statement

**Francisco Fiol:** Conceptualization, Methodology, Investigation, Data curation. **Víctor Revilla-Cuesta:** Data curation, Software, Writing – original draft, Writing – review & editing. **Carlos Thomas:** Supervision, Writing – review & editing, Resources, Funding acquisition. **Juan M. Manso:** Supervision, Writing – review & editing, Resources, Funding acquisition.

## Declaration of Competing Interest

The authors declare that they have no known competing financial interests or personal relationships that could have appeared to influence the work reported in this paper.

## Data availability

Data will be made available on request.

## Acknowledgements

This research work was supported by the Spanish Ministry of Universities, MICINN, AEI, EU, ERDF and NextGenerationEU/PRTR [grant numbers PID2020-113837RB-I00; 10.13039/501100011033; TED2021-129715B-I00]; the Junta de Castilla y León (Regional Government) and ERDF [grant number UIC-231]; and, finally, the University of Burgos [grant number SUCONS, Y135.GI].

## References

- [1] D. Domínguez-Santos, Structural performance of concrete blocks with wood aggregates for the construction of medium and high-rise buildings, *Inf. Constr.* 73 (564) (2021) e414.
- [2] A.A. Abdulhameed, A.N. Hanoon, H.A. Abdulhameed, Q.S. Banyhussan, A. S. Mansi, Push-out test of steel-concrete-steel composite sections with various core materials: behavioural study, *Arch. Civ. Mech. Eng.* 21 (1) (2021) 17, <https://doi.org/10.1007/s43452-021-00173-y>.
- [3] P. Busch, A. Kendall, C.W. Murphy, S.A. Miller, Literature review on policies to mitigate GHG emissions for cement and concrete, *Resour. Conserv. Recycl.* 182 (2022), 106278, <https://doi.org/10.1016/j.resconrec.2022.106278>.
- [4] L.J. Drew, W.H. Langer, J.S. Sachs, Environmentalism and natural aggregate mining, *Nat. Resour. Res.* 11 (1) (2002) 19–28, <https://doi.org/10.1023/A:1014283519471>.
- [5] N.R. Mohanta, M. Murmu, Alternative coarse aggregate for sustainable and eco-friendly concrete - A review, *J. Build. Eng.* 59 (2022), 105079, <https://doi.org/10.1016/j.jobe.2022.105079>.
- [6] A.M.D. Souza, J.M. Franco de Carvalho, C.F.R. Santos, F.A. Ferreira, L.G. Pedroti, R.A.F. Peixoto, On the strategies to improve the eco-efficiency of self-compacting concrete using industrial waste: An analytical review, *Constr. Build. Mater.* 347 (2022), 128634, <https://doi.org/10.1016/j.conbuildmat.2022.128634>.
- [7] Y.A. Villagrán-Zaccardi, A.T.M. Marsh, M.E. Sosa, C.J. Zega, N. De Belie, S. A. Bernal, Complete re-utilization of waste concretes-Valorisation pathways and research needs, *Resour. Conserv. Recycl.* 177 (2022), 105955, <https://doi.org/10.1016/j.resconrec.2021.105955>.
- [8] Z.H. He, H.N. Zhu, M.Y. Zhang, J.Y. Shi, S.G. Du, B. Liu, Autogenous shrinkage and nano-mechanical properties of UHPC containing waste brick powder derived from construction and demolition waste, *Constr. Build. Mater.* 306 (2021), 124869, <https://doi.org/10.1016/j.conbuildmat.2021.124869>.
- [9] M. Etxeberria, M. Konoiko, C. García, M.Á. Pérez, Water-washed fine and coarse recycled aggregates for real scale concretes production in barcelona, *Sustainability* 14 (2) (2022) 708, <https://doi.org/10.3390/su14020708>.
- [10] Z.H. He, X.D. Han, M.Y. Zhang, Q. Yuan, J.Y. Shi, P.M. Zhan, A novel development of green UHPC containing waste concrete powder derived from construction and demolition waste, *Powder Technol.* 398 (2022), 117075, <https://doi.org/10.1016/j.powtec.2021.117075>.
- [11] B. Li, S. Hou, Z. Duan, L. Li, W. Guo, Rheological behavior and compressive strength of concrete made with recycled fine aggregate of different size range, *Constr. Build. Mater.* 268 (2021), 121172, <https://doi.org/10.1016/j.conbuildmat.2020.121172>.
- [12] F. Faleschini, M.A. Zanini, L. Hofer, Reliability-based analysis of recycled aggregate concrete under carbonation, *Adv. Civ. Eng.* 2018 (2018) 4742372, <https://doi.org/10.1155/2018/4742372>.
- [13] J.J. Xu, Z.P. Chen, T. Ozbakkaloglu, X.Y. Zhao, C. Demartino, A critical assessment of the compressive behavior of reinforced recycled aggregate concrete columns, *Eng. Struct.* 161 (2018) 161–175, <https://doi.org/10.1016/j.engstruct.2018.02.003>.
- [14] L. Evangelista, J. De Brito, Concrete with fine recycled aggregates: A review, *Eur. J. Environ. Civ. Eng.* 18 (2) (2014) 129–172, <https://doi.org/10.1080/19648189.2013.851038>.
- [15] F. Yu, X. Li, J. Song, Y. Fang, Y. Qin, S. Bu, Experimental study on flexural capacity of PVA fiber-reinforced recycled concrete slabs, *Arch. Civ. Mech. Eng.* 21 (4) (2021) 166, <https://doi.org/10.1007/s43452-021-00314-3>.
- [16] C. Feng, B. Cui, Y. Huang, H. Guo, W. Zhang, J. Zhu, Enhancement technologies of recycled aggregate – Enhancement mechanism, influencing factors, improvement effects, technical difficulties, life cycle assessment, *Constr. Build. Mater.* 317 (2022), 126168, <https://doi.org/10.1016/j.conbuildmat.2021.126168>.
- [17] J.J. Xu, W.G. Chen, C. Demartino, T.Y. Xie, Y. Yu, C.F. Fang, M. Xu, A Bayesian model updating approach applied to mechanical properties of recycled aggregate concrete under uniaxial or triaxial compression, *Constr. Build. Mater.* 301 (2021), 124274, <https://doi.org/10.1016/j.conbuildmat.2021.124274>.
- [18] B. Xiong, C. Demartino, J. Xu, A. Simi, G.C. Marano, Y. Xiao, High-strain rate compressive behavior of concrete made with substituted coarse aggregates: Recycled crushed concrete and clay bricks, *Constr. Build. Mater.* 301 (2021), 123875, <https://doi.org/10.1016/j.conbuildmat.2021.123875>.
- [19] X.Y. Zhao, J.X. Chen, G.M. Chen, J.J. Xu, L.W. Zhang, Prediction of ultimate condition of FRP-confined recycled aggregate concrete using a hybrid boosting model enriched with tabular generative adversarial networks, *Thin-Walled Struct.* 182 (2023), 110318, <https://doi.org/10.1016/j.tws.2022.110318>.
- [20] V. Revilla-Cuesta, V. Ortega-López, M. Skaf, F. Fiol, J.M. Manso, Why is the effect of recycled concrete aggregate on the compressive strength of self-compacting concrete not homogeneous? A bibliographic review, *Inf. Constr.* 74 (565) (2022) e435.
- [21] W. Chen, J. Xu, Z. Li, X. Huang, Y. Wu, Load-carrying capacity of circular recycled aggregate concrete-filled steel tubular stub columns under axial compression: Reliability analysis and design factor calibration, *J. Build. Eng.* 66 (2023), 105935, <https://doi.org/10.1016/j.jobe.2023.105935>.
- [22] F. Fiol, C. Thomas, C. Muñoz, V. Ortega-López, J.M. Manso, The influence of recycled aggregates from precast elements on the mechanical properties of structural self-compacting concrete, *Constr. Build. Mater.* 182 (2018) 309–323, <https://doi.org/10.1016/j.conbuildmat.2018.06.132>.
- [23] F. Fiol, C. Thomas, J.M. Manso, I. López, Transport mechanisms as indicators of the durability of precast recycled concrete, *Constr. Build. Mater.* 269 (2021), 121263, <https://doi.org/10.1016/j.conbuildmat.2020.121263>.
- [24] S.A. Santos, P.R. da Silva, J. de Brito, Self-compacting concrete with recycled aggregates – A literature review, *J. Build. Eng.* 22 (2019) 349–371, <https://doi.org/10.1016/j.jobe.2019.01.001>.
- [25] H.A. Bulut, R. Şahin, Radiological characteristics of Self-Compacting Concretes incorporating fly ash, silica fume, and slag, *J. Build. Eng.* 58 (2022), 104987, <https://doi.org/10.1016/j.jobe.2022.104987>.
- [26] M. Ouchi, Y. Edamatsu, K. Ozawa, H. Okamura, Simple evaluation method for interaction between coarse aggregate and mortar's particles in self-compacting concrete, *Trans. Jpn. Concr. Inst.* 21 (1999) 1–6.
- [27] V. Revilla-Cuesta, V. Ortega-López, M. Skaf, A.U.R. Khan, J.M. Manso, Deformational behavior of self-compacting concrete containing recycled aggregate, slag cement and green powders under compression and bending: Description and prediction adjustment, *J. Build. Eng.* 54 (2022), 104611, <https://doi.org/10.1016/j.jobe.2022.104611>.
- [28] N. Bahrami, M. Zohrabi, S.A. Mahmoudy, M. Akbari, Optimum recycled concrete aggregate and micro-silica content in self-compacting concrete: Rheological, mechanical and microstructural properties, *J. Build. Eng.* 31 (2020), 101361, <https://doi.org/10.1016/j.jobe.2020.101361>.
- [29] J.Y. Hu, S.S. Zhang, E. Chen, W.G. Li, A review on corrosion detection and protection of existing reinforced concrete (RC) structures, *Constr. Build. Mater.* 325 (2022), 126718, <https://doi.org/10.1016/j.conbuildmat.2022.126718>.
- [30] A.A. Bahraq, J. Jose, M. Shameem, M. Maslehuddin, A review on treatment techniques to improve the durability of recycled aggregate concrete: Enhancement mechanisms, performance and cost analysis, *J. Build. Eng.* 55 (2022), 104713, <https://doi.org/10.1016/j.jobe.2022.104713>.
- [31] X. Zheng, Y. Wang, S. Zhang, F. Xu, X. Zhu, X. Jiang, L. Zhou, Y. Shen, Q. Chen, Z. Yan, W. Zhao, H. Zhu, Y. Zhang, Research progress of the thermophysical and mechanical properties of concrete subjected to freeze-thaw cycles, *Constr. Build. Mater.* 330 (2022), 127254, <https://doi.org/10.1016/j.conbuildmat.2022.127254>.
- [32] S. Luo, T. Bai, M. Guo, Y. Wei, W. Ma, Impact of freeze-thaw cycles on the long-term performance of concrete pavement and related improvement measures: A review, *Materials* 15 (13) (2022) 4568, <https://doi.org/10.3390/ma15134568>.
- [33] S.A. Santos, P.R. Da Silva, J. De Brito, Durability evaluation of self-compacting concrete with recycled aggregates from the precast industry, *Mag. Concr. Res.* 71 (24) (2019) 1265–1282, <https://doi.org/10.1680/jmacr.18.00225>.
- [34] H.B. Hu, Z.H. He, J.Y. Shi, C.F. Liang, T.G. Shibro, B.J. Liu, S.Y. Yang, Mechanical properties, drying shrinkage, and nano-scale characteristics of concrete prepared with zeolite powder pre-coated recycled aggregate, *J. Clean. Prod.* 319 (2021), 128710, <https://doi.org/10.1016/j.jclepro.2021.128710>.
- [35] H.B. Hu, Z.H. He, K.J. Fan, T.G. Shibro, B.J. Liu, J.Y. Shi, Properties enhancement of recycled coarse aggregates by pre-coating/pre-soaking with zeolite powder/calcium hydroxide, *Constr. Build. Mater.* 286 (2021), 122888, <https://doi.org/10.1016/j.conbuildmat.2021.122888>.
- [36] V. Revilla-Cuesta, F. Faleschini, M.A. Zanini, M. Skaf, V. Ortega-López, Porosity-based models for estimating the mechanical properties of self-compacting concrete with coarse and fine recycled concrete aggregate, *J. Build. Eng.* 44 (2021), 103425, <https://doi.org/10.1016/j.jobe.2021.103425>.
- [37] G.N. Gopu, S.A. Joseph, Corrosion Behavior of Fiber-Reinforced Concrete—A Review, *Fibers* 10 (5) (2022) 38, <https://doi.org/10.3390/fib10050038>.

- [38] J.R. Bone, R. Stafford, A.E. Hall, R.J.H. Herbert, The intrinsic primary bioreceptivity of concrete in the coastal environment – A review, *Dev. Built. Environ.* 10 (2022), 100078, <https://doi.org/10.1016/j.dibe.2022.100078>.
- [39] A. Santamaría, A. Orbe, J.T. San José, J.J. González, A study on the durability of structural concrete incorporating electric steelmaking slags, *Constr. Build. Mater.* 161 (2018) 94–111, <https://doi.org/10.1016/j.conbuildmat.2017.11.121>.
- [40] V. Ortega-López, F. Faleschini, C. Pellegrino, V. Revilla-Cuesta, J.M. Manso, Validation of slag-binder fiber-reinforced self-compacting concrete with slag aggregate under field conditions: Durability and real strength development, *Constr. Build. Mater.* 320 (2022), 126280, <https://doi.org/10.1016/j.conbuildmat.2021.126280>.
- [41] W. Chalee, T. Cheewaket, C. Jaturapitakkul, Utilization of recycled aggregate concrete for marine site based on 7-year field monitoring, *Ind. J. Concr. Struct. Mater.* 15 (1) (2021) 34, <https://doi.org/10.1186/s40069-021-00473-w>.
- [42] EN-Euronorm, Rue de stassart, 36. Belgium-1050 Brussels, European Committee for Standardization.
- [43] EFNARC, Specification Guidelines for Self-compacting Concrete, European Federation of National Associations Representing producers and applicators of specialist building products for Concrete (2002).
- [44] C. Thomas, J. Setién, J.A. Polanco, P. Alaejos, M. Sánchez De Juan, Durability of recycled aggregate concrete, *Constr. Build. Mater.* 40 (2013) 1054–1065, <https://doi.org/10.1016/j.conbuildmat.2012.11.106>.
- [45] D. Carro-López, B. González-Fontebao, J. De Brito, F. Martínez-Abella, I. González-Taboada, P. Silva, Study of the rheology of self-compacting concrete with fine recycled concrete aggregates, *Constr. Build. Mater.* 96 (2015) 491–501, <https://doi.org/10.1016/j.conbuildmat.2015.08.091>.
- [46] UNE 83966, Concrete durability. Test methods. Conditioning of concrete test pieces for the purpose of gas permeability and capillary suction tests (2008).
- [47] UNE 83982, Concrete durability. Test methods. Determination of the capillary suction in hardened concrete. Fagerlund method (2008).
- [48] B. Cantero, M. Bravo, J. de Brito, I.F. Sáez del Bosque, C. Medina, Water transport and shrinkage in concrete made with ground recycled concrete-added cement and mixed recycled aggregate, *Cem. Concr. Compos.* 118 (2021), 103957, <https://doi.org/10.1016/j.cemconcomp.2021.103957>.
- [49] P. Deng, Z. Cong, Y. Liu, Y. Huang, Q. Zhu, Effect of dry-wet cycles on BFRP bars and modified ceramsite concrete in marine environments, *J. Mater. Civ. Eng.* 34 (7) (2022) 04022125, [https://doi.org/10.1061/\(ASCE\)MT.1943-5533.0004273](https://doi.org/10.1061/(ASCE)MT.1943-5533.0004273).
- [50] EC-2, Eurocode 2: Design of concrete structures. Part 1-1: General rules and rules for buildings, CEN (European Committee for Standardization) (2010).
- [51] S.N. Londhe, P.S. Kulkarni, P.R. Dixit, A. Silva, R. Neves, J. de Brito, Predicting carbonation coefficient using Artificial neural networks and genetic programming, *J. Build. Eng.* 39 (2021), 102258, <https://doi.org/10.1016/j.job.2021.102258>.
- [52] I. Ocampo, O. Vuanello, R. Ortíz, H. Seminario, G. Paez, I. Ibarbe, S. Bustos, R. Vila, Estudio de la carbonatación acelerada en probetas de hormigón armado VI Congreso Internacional sobre Patología y Recuperación de Estructuras (2010).
- [53] Structural Code, Código Estructural de España. Spanish Structural Code, Ministerio de Fomento, Gobierno de España (2021).
- [54] V.G. Papadakis, M.N. Fardis, C.G. Vayenas, Hydration and carbonation of pozzolanic cements, *ACI Mater. J.* 89 (2) (1992) 119–130.
- [55] V.G. Papadakis, M.N. Fardis, C.G. Vayenas, Effect of composition, environmental factors and cement-lime mortar coating on concrete carbonation, *Mater. Struct.* 25 (5) (1992) 293–304, <https://doi.org/10.1007/BF02472670>.
- [56] V.L. Ta, S. Bonnet, T. Senga Kiese, A. Ventura, A new meta-model to calculate carbonation front depth within concrete structures, *Constr. Build. Mater.* 129 (2016) 172–181, <https://doi.org/10.1016/j.conbuildmat.2016.10.103>.
- [57] L. Parrot, Design for avoiding damage due to carbonation-induced corrosion, *Am. Concr. Inst. ACI Spec. Publ. SP-145* (1994) 283–298.
- [58] C. Thomas, J. Setién, J.A. Polanco, Structural recycled aggregate concrete made with precast wastes, *Constr. Build. Mater.* 114 (2016) 536–546, <https://doi.org/10.1016/j.conbuildmat.2016.03.203>.
- [59] A. Gonzalez-Corominas, M. Etxeberria, Effects of using recycled concrete aggregates on the shrinkage of high performance concrete, *Constr. Build. Mater.* 115 (2016) 32–41, <https://doi.org/10.1016/j.conbuildmat.2016.04.031>.
- [60] G. Puente de Andrade, G. de Castro Polisseni, M. Pepe, R.d., Toledo Filho, Design of structural concrete mixtures containing fine recycled concrete aggregate using packing model, *Constr. Build. Mater.* 252 (2020), 119091, <https://doi.org/10.1016/j.conbuildmat.2020.119091>.
- [61] J. Bao, S. Li, P. Zhang, X. Ding, S. Xue, Y. Cui, T. Zhao, Influence of the incorporation of recycled coarse aggregate on water absorption and chloride penetration into concrete, *Constr. Build. Mater.* 239 (2020), 117845, <https://doi.org/10.1016/j.conbuildmat.2019.117845>.
- [62] K. Zhang, J. Xiao, Y. Hou, Q. Zhang, Experimental study on carbonation behavior of seawater sea sand recycled aggregate concrete, *Adv. Struct. Eng.* 25 (5) (2022) 927–938, <https://doi.org/10.1177/13694332211026221>.
- [63] S. Uthaman, V. Vishwakarma, R.P. George, D. Ramachandran, K. Kumari, R. Preetha, M. Premila, R. Rajaraman, U.K. Mudali, G. Amarendra, Enhancement of strength and durability of fly ash concrete in seawater environments: Synergistic effect of nanoparticles, *Constr. Build. Mater.* 187 (2018) 448–459.
- [64] Q. Al-Waked, J. Bai, J. Kinuthia, P. Davies, Enhancing the aggregate impact value and water absorption of demolition waste coarse aggregates with various treatment methods, *Case Stud. Constr. Mater.* 17 (2022) e01267.
- [65] N. Singh, S.P. Singh, Evaluating the performance of self compacting concretes made with recycled coarse and fine aggregates using non destructive testing techniques, *Constr. Build. Mater.* 181 (2018) 73–84, <https://doi.org/10.1016/j.conbuildmat.2018.06.039>.
- [66] M.T. Blanco-Varela, J. Aguilera, S. Martínez-Ramírez, A. Palomo, C. Sabbioni, C. Riontino, G. Zappia, K. Vanvalen, E.E. Toubakari, Thaumassite formation in hydraulic mortars by atmospheric SO<sub>2</sub> deposition, *Mater. Constr.* 2001 (263–264) (2001) 109–125, <https://doi.org/10.3989/mc.2001.v51.i263-264.357>.
- [67] V. Ortega-López, J.A. Fuente-Alonso, A. Santamaría, J.T. San-José, A. Aragón, Durability studies on fiber-reinforced EAF slag concrete for pavements, *Constr. Build. Mater.* 163 (2018) 471–481, <https://doi.org/10.1016/j.conbuildmat.2017.12.121>.
- [68] ASTM-International, Book Annual of ASTM Standards, West Conshohocken, 19429–2959 2008 USA PA. (2008).
- [69] F. Fiol, C. Thomas, J.M. Manso, I. López, Influence of recycled precast concrete aggregate on durability of concrete's physical processes, *Appl. Sci.* 10 (20) (2020) 7348, <https://doi.org/10.3390/app10207348>.
- [70] I. Sosa, P. Tamayo, J.A. Sainz-Aja, C. Thomas, J. Setién, J.A. Polanco, Durability aspects in self-compacting siderurgical aggregate concrete, *J. Build. Eng.* 39 (2021), 102268, <https://doi.org/10.1016/j.job.2021.102268>.
- [71] R.K. Dhir, M.C. Limbachiya, T. Leelawat, Suitability of recycled concrete aggregate for use in BS 5328 designated mixes, *Proc. Inst. Civ. Eng. Struct. Build.* 134 (3) (1999) 257–274.